Eur Biophys J (2010) 39:1193–1205
DOI 10.1007/s00249-009-0571-5

ORIGINAL PAPER

Camptosemin, a tetrameric lectin of *Camptosema ellipticum*: structural and functional analysis

Fernanda A. H. Batista · Leandro S. Goto · Wanius Garcia · Derminda I. de Moraes · Mario de Oliveira Neto · Igor Polikarpov · Marcia R. Cominetti · Heloísa S. Selistre-de-Araújo · Leila M. Beltramini · Ana Paula Ulian Araújo

Received: 26 August 2009 / Revised: 3 December 2009 / Accepted: 14 December 2009 / Published online: 3 January 2010

Abstract Lectins have been classified into a structurally diverse group of proteins that bind carbohydrates and glycoconjugates with high specificity. They are extremely useful molecules in the characterization of saccharides, as drug delivery mediators, and even as cellular surface makers. In this study, we present camptosemin, a new lectin from *Camptosema ellipticum*. It was characterized as an *N*-acetyl-D-galactosamine-binding homo-tetrameric lectin, with a molecular weight around 26 kDa/monomers. The monomers were stable over a wide range of pH values and exhibited pH-dependent oligomerization. Camptosemin promoted adhesion of breast cancer cells and hemagglutination, and both activities were inhibited by its binding of sugar. The stability and unfolding/folding behavior of this lectin was characterized using fluorescence and far-UV circular dichroism spectroscopies. The results indicate that chemical unfolding of camptosemin proceeds as a two-state monomer-tetramer process. In addition, small-angle X-ray scattering shows that camptosemin behaves as a soluble and stable homo-tetramer molecule in solution.

Keywords Lectin · Camptosemin · CD spectroscopy · Fluorescence spectroscopy · Refolding · SAXS

F. A. H. Batista and L. S. Goto contributed equally to this work.

F. A. H. Batista · L. S. Goto · W. Garcia · D. I. de Moraes · M. de Oliveira Neto · I. Polikarpov · L. M. Beltramini · A. P. U. Araújo
Centro de Biotecnologia Molecular Estrutural (CBME), Instituto de Física de São Carlos (IFSC), Universidade de São Paulo (USP), São Carlos, Brazil

F. A. H. Batista · A. P. U. Araújo
Programa de Pós-graduação em Genética e Evolução, Universidade Federal de São Carlos (UFSCar), São Carlos, Brazil

M. R. Cominetti · H. S. Selistre-de-Araújo
Departamento de Ciências Fisiológicas, Universidade Federal de São Carlos (UFSCar), São Carlos, Brazil

A. P. U. Araújo (✉)
Grupo de Biofísica Molecular "Sérgio Mascarenhas", Instituto de Física de São Carlos, Universidade de São Paulo, Caixa Postal 369, São Carlos 13560-970, Brazil
e-mail: anapaula@ifsc.usp.br

Introduction

Lectins are proteins of non-immune origin with the ability to bind carbohydrates in a reversible way. Although widely distributed in nature, the plant-isolated lectins are the most extensively studied, being found in roots, bulbs, bark, and leaves (Rüdiger and Gabius 2001). Lectins have been studied extensively in recent years because of their usefulness as molecular tools in investigations of cell surface composition/changes, growth, differentiation, and aggregation, as well as in studies of several pathological mechanisms and in the isolation and characterization of glycoconjugates (Sharon and Lis 2004; Sharon 2007). Despite the existence of many studies about lectin-carbohydrate interactions reported in the literature, relatively little information is known about their stability and the folding of multimeric lectins (Campana et al. 2002; Chatterjee and Mandal 2003).

Plant lectins can be structurally and evolutionarily classified into seven protein families; among these, the family of legume lectins is well characterized, with several examples isolated from different species (Gatehouse et al. 1995; Van Damme et al. 1998). The legume lectin family is composed of closely related proteins, found exclusively in

specimens of the Leguminoseae family (Fabaceae; Sharon and Lis 1990).

Structurally, legume lectins present high sequential identity, and the monomers share the same tertiary structure, which is characterized by an essentially conserved "jelly roll" motif, consisting of three sets of antiparallel β-sheets connected by loops of diverse sizes: a flat six-stranded back β-sheet, a curved seven-membered front β-sheet, and a five-membered top β-sheet (Loris et al. 1998). The oligomerization process of these proteins involves the six-stranded back β-sheet in various ways, and the resulting mutual disposition of these β-sheets in the participating monomers leads to diverse quaternary structures (Chatterjee and Mandal 2005). Most legume lectins are known to exist as homodimers or homotetramers, and even though all the monomers have a similar tertiary structure, their modes of quaternary association are highly variable (Brinda et al. 2004). The consensus is that the quaternary structure causes the lectin to exhibit multivalent binding to cells, which is necessary for its biological activity. These molecules have recently been chosen as model systems for investigating how oligomeric proteins drive folding and to study the association of subunits (Chatterjee and Mandal 2003; Chatterjee and Mandal 2005). Also, the conformational stability of a protein gives a means to elucidate the nature of the forces that contribute to its folding, which is essential for maintenance of its functionality (Sinha et al. 2005).

In the present paper, we report the isolation, structural and functional characterization, oligomerization, and unfolding/refolding studies of native camptosemin, a tetrameric lectin from seeds of *Camptosema ellipticum*. This species belongs to the Phaseolae tribe of the Leguminosae family (Varela et al. 2004); this is the first time that a lectin from this genus has been studied. Our investigation includes the protein purification, molecular cloning, and structural aspects like folding/unfolding behavior, thermodynamic properties, and oligomerization states. Additionally, the ability of camptosemin to promote adhesion of MDA-MB-231 breast tumor cells and to bind to selective sugars was investigated.

Materials and methods

Materials

Seeds of *C. ellipticum* (Desv.) Burkart were collected from plants growing around São Carlos-SP (Brazil) (geodesic coordinates S 21°54′52.6″ and W 47°48′57.5″). Columns and resins were purchased from Amersham Pharmacia Biotech (GE-Healthcare). All other chemical reagents used in this study were analytical grade, unless otherwise specified.

Isolation and purification

Mature *C. ellipticum* seeds were ground, added to PBS (pH 7.4), 1:5 (w/v) and incubated for 2 h at 4°C. After incubation, centrifugation at 10,000×*g* for 20 min at 4°C was carried out, and the supernatant was filtered and denoted as crude extract. Even though immobilized lactose affinity chromatography based purifications attempts were successful, such an approach only gave a low protein yield. Thus, we found an alternative purification methodology. The lectin from crude extract was separated by size exclusion chromatography (SEC) on a Superdex-75 10/300 GL column coupled to an ÄKTA purifier system (Amersham Pharmacia Biotech). The column had previously been equilibrated with PBS, and protein elution was performed using the same buffer (flow rate of 0.5 ml/min and collection of 1 ml fractions, monitored by absorbance at 280 nm). Fractions exhibiting hemagglutinating activity were pooled, concentrated by filtration on a Centriprep-10 (Amicon), and reloaded onto the same column. A second SEC elution was carried out with PBS buffer plus lactose 0.2 M. The fractions from the last SEC that showed hemagglutinating activity were pooled, concentrated in a Centriprep-10, and loaded onto a Mono-Q 5/50 GL (Amersham Biosciences) column coupled to the ÄKTA purifier system. The column had previously been equilibrated with 20 mM Tris–HCl buffer, pH 8.0. Elution was performed with the same buffer, using a linear gradient of 0–1 M NaCl (flow rate of 1 ml/min). The fractions exhibiting hemagglutinating activity were collected and analyzed by SDS-PAGE (Laemmli 1970). Protein concentrations were determined by BCA Protein Assay Reagent (Pierce).

Biological activity: hemagglutination

Hemagglutination activity was measured on microagglutination plates, using a 2% suspension of human erythrocytes of each ABO group. The extent of agglutination of a series of 1:2 protein dilutions (initial protein concentration of 4.5 μM) was monitored visually after 30 min of incubation. The activity is defined as the minimum amount of protein that still promoted visible agglutination.

Inhibition of hemagglutination induced by sugar

The lectin specificities of eight different saccharides were determined by inhibition of hemagglutinating activity: sucrose 1.0 M, maltose 1.0 M, lactose 0.5 M, galactose 1.0 M, mannose 1.0 M, melibiose 0.5 M, Me-α-D-galactopyranoside 1.0 M, and *N*-acetyl-D-galactosamine 1.0 M. The assay was performed using 25 μl of a two-fold serial dilution of each sugar, added to 25 μl of lectin solution in PBS (3 μM of camptosemin) and incubated for 30 min.

After incubation, 50 µl of a 2% suspension of erythrocytes (O group) in PBS was added to each well and incubated. After 2 h of incubation, the inhibition was evaluated visually and compared to controls. The minimum concentration of sugar that completely inhibited the lectin-induced hemagglutination was defined to be the minimal inhibitory sugar concentration (MIC).

Cell adhesion and cell adhesion inhibition assays using MDA-MB-231 breast cancer cells

Frozen cell stocks were inoculated in 75 cm^2 cell culture bottles containing 10 ml of DMEM supplemented with 10% FBS, penicillin 100 U/ml, and streptomycin 100 µg/ml. Cells were cultivated at 37°C in a 5% CO_2 atmosphere until they achieved 90% confluence. Adhered cells were detached by incubation for 5 min in 5 ml of 0.25% trypsin in PBS (50 mM phosphate buffer, pH 7.4, 0.5 mM EDTA, 150 mM NaCl). Adhesion assays were performed as previously described (Cominetti et al. 2004). Briefly, cell suspensions were adjusted to 5×10^6 cells/ml in an adhesion buffer (20 mM HEPES, pH 7.4, 150 mM NaCl, 5 mM KCl, 1 mM $MnCl_2$, 1 mM $MgSO_4$), and CMFDA was added to a final concentration of 12.5 µM. Cells were incubated for 30 min at 37°C and then washed three times with adhesion buffer. The cell suspension was adjusted to 10^6 cells/ml. Camptosemin (10 µg) was incubated with GalNAc for 1 h at room temperature at molar ratios from 1:1 to 1:32 (camptosemin: GalNAc) in adhesion buffer. The mixture was dispensed into flat-bottom 96-well plates and incubated overnight at 4°C. The negative controls were composed of 100 µl of a solution of 1% bovine serum albumin (BSA) in the same buffer. Positive controls were composed of 100 µl of collagen type I, at 10 µg/µl. After incubation, each well was poured out and blocked with 200 µl of 1% BSA in adhesion buffer for 2 h at room temperature, followed by three wash steps with adhesion buffer. Labeled cell suspensions were dispensed into the coated wells (100 µl) and incubated for 30 min at 37°C. After the unbound cells were washed away, the bound cells were lysed by the addition of 0.5% Triton X-100. The plates were read using a SpectraMax Gemini XS fluorescence plate reader (Molecular Devices, Sunnyvale, CA) with a 485-nm excitation and a 530-nm emission filter. Each experiment was performed in triplicate, and the mean values were plotted and normalized as percentage values of the positive controls.

cDNA cloning

Plant RNA extraction

Total RNA was isolated from immature seeds of *C. ellipticum*, which had previously been frozen in liquid nitrogen, using the RNA*easy Plant Mini* Kit (Qiagen). The RNA was quantified by measuring absorption at 260 nm with a Hitachi U-2000 spectrophotometer.

cDNA isolation

The partial fragment that encodes camptosemin was amplified, using a degenerated oligonucleotide, by RT-PCR. The synthesis of the first strand of cDNA was performed using 1 µg of total RNA from *C. ellipticum,* 100 pmol of the oligo-dT reverse primer, and 0.4 mM dNTPs, in the manufacturer-recommended *AMV/Tf/Reaction Buffer*. The mixture was heated to 70°C for 5 min, followed by cooling in an ice-bath and addition of 200 U of *AMV Reverse Transcriptase* (Promega) and incubation at 48°C for 1 h. The first strand was purified by ethanol precipitation. The nucleic acid was recovered by centrifugation at 16,000×*g* for 5 min and then washed in 70% ethanol, air dried, and suspended in sterile water. The PCR to amplify the fragment encoding camptosemin was performed using the cDNA obtained as described above adding 100 pmol of each primer (Camp-fw2 and oligo-dT_{15}-Promega), 0.4 mM dNTP, 2.5 mM $MgSO_4$, *High Fidelity PCR Buffer* and 2.5 U of *High Fidelity PCR Enzyme Mix* (Fermentas), and water to 25 µl. The first primer sequence, Camp-fw2 (5′ ATHAARYTNCARGGN AAYGC 3′), corresponds to minor degeneration and the major confiability region of the camptosemin N-terminal sequence (IKLQGNAA). The amplification was performed in an Eppendorf Mastercycler (Eppendorf) under the following conditions: one cycle at 94°C for 3 min, 10 cycles at 94°C for 1 min, 42°C for 1 min, 72°C for 3 min, and 40 cycles at 94°C for 1 min, 45°C for 1 min, 72°C for 3 min, and 72°C for 7 min in a final extension. The final product was purified using the *Wizard SV Gel and PCR Clean-Up System* kit (Promega), inserted into the Topo TA cloning vector (Invitrogen), and propagated in *E. coli* DH5α strain. Sequencing (Sanger et al. 1977) was performed in an ABI Prism 377 automated DNA sequencer (Perkin Elmer), following the manufacturer's protocol. The obtained sequence encoding camptosemin was submitted to the BLAST script databank search (Altschul et al. 1997).

5′-RACE (rapid amplification of cDNA ends)

The 5′-RACE was performed according to an adapted protocol, described previously (Frohman et al. 1988). The specific primer for 5′-RACE was: CampRACE_External: 5′CTGGGTGTCCTGAGGTGCAAG3′ for 5′cDNA extension, and CampRACE_Internal: 5′GCAACATTGCCGGT GGCTTC3′. Terminal transferase (Invitrogen) was used to add a homopolymer G-tail to the first strand product from 5′-RACE. In the amplification of the 5′cDNA by PCR, we

used CampRACE_Internal and a poli-C oligonucleotide primer. The PCR product was purified using *Wizard SV Gel and PCR Clean-Up System* (Promega), inserted into the pCR 2.1 vector (*TopoTA cloning,* Invitrogen), and propagated in *E. coli* DH5α cells. Recombinant clones were subjected to plasmidial extraction and sequencing as described above.

Structural characterization studies

The molecular mass (MM) of camptosemin was estimated by 15% SDS–PAGE (Laemmli 1970), with and without heating, and in the presence or absence of β-mercaptoethanol. N-terminal analyses were performed in the PPSQ-231 Shimadzu automatic protein sequencer (Kyoto, Japan), following the manufacturer's recommendations. The percentage of sequence identity with lectins from the legume lectin family was determined using the NCBI-BLAST (Altschul et al. 1997) databank and multiple sequence alignment, performed with CLUSTAL W (Larkin et al. 2007).

Size exclusion chromatography (SEC)

The apparent molecular mass of camptosemin was estimated with size exclusion chromatography on a Superdex-200 10/300 GL column (Amersham Biosciences) driven by an ÄKTA purifier system (Amersham Pharmacia Biotech). The column was equilibrated with 20 mM Tris–HCl buffer, pH 8.0, containing 0.2 M lactose and 0.3 M NaCl. The presence of 0.3 M salt in SEC experiments was used to avoid any protein unspecific interactions with the chromatographic matrix. Additionally, it is known that if no sugar is in the buffer, lectins usually exhibit an elution delay due to interactions with the polysaccharide column matrix, and no reliable estimate of native protein Mr can be obtained by SEC. To prevent this, we used 0.2 M lactose in the buffer. The molecular mass standards were β-amilase (200 kDa), alcohol dehydrogenase (150 kDa), bovine serum albumin (66 kDa), carbonic anhydrase (30 kDa), and cytochrome C (12 kDa) (Sigma–Aldrich). The apparent molecular mass of camptosemin was determined from the calibration curve (K_{av} vs. log[MW]), with K_{av} determined by: K_{av} = (elution volume − column void volume)/(geometric column volume − column void volume).

Circular dichroism spectroscopy (CD)

Far-UV CD spectroscopy (195–250 nm) was performed using a J-715 Jasco spectropolarimeter equipped with a temperature control device. Sixteen accumulations were averaged to form the CD spectra, taken using a scanning speed of 100 nm min^{-1}, a spectral bandwidth of 1 nm, and a response time of 0.5 s, and obtained on degree scale. The camptosemin concentrations were approximately 9.0 and 19.5 μM in 20 mM Tris–HCl buffer, pH 8.0, containing 20 mM NaCl. Quartz cuvettes, 1 mm in path length, were used for the far-UV CD measurements at 20°C. The buffer contribution was subtracted in each of the experiments. The CLUSTER program was used to determine the tertiary structure class, based on the protein CD spectra (Sreerama et al. 2001).

Small-angle X-ray scattering (SAXS)

The small-angle X-ray scattering experiments on the camptosemin at 52.0 and 315.0 μM molar concentrations (in 20 mM Tris-HCl pH 8.0 buffer, containing 20 mM NaCl) were carried out at the LNLS (National Synchrotron Light Laboratory, Campinas, Brazil) synchrotron SAXS beamline. The samples were centrifuged for 10 min at 13,000×*g* (at 4°C) prior to the measurements. The wavelength of the incoming monochromatic X-ray beam was set to $\lambda = 0.148$ nm. A 1D X-ray position sensitive detector (PSD) was utilized to record the scattering intensity as a function of scattering angle. Parasitic scattering from the air and the beamline windows was subtracted from the total measured intensities. Desmearing of the experimental results was performed since the entrance window of the 1D PSD was 8 mm high. The sample-to-detector distance (732.1 mm) was adjusted in order to record the scattering intensity over a range of q values from 0.01 to 2.35 nm^{-1}. The samples were loaded into cells made of two thin parallel mica windows and kept at 20°C during the measurements. The scattering curves of the protein solutions and the corresponding solvents were collected in 20 frames of 100 s each, to monitor radiation damage and beam stability. The data were normalized to the intensity of the incident beam and corrected for detector response. The scattering of the buffer was subtracted, and the difference curves were scaled for concentration. Data analysis was performed using the GNOM program package (Svergun et al. 1988; Svergun 1992). Ab initio model simulations were performed using the program GASBOR (Svergun et al. 2001; Petoukhov and Svergun 2003). At least ten independent dummy atom model (DAM) reconstructions, starting from random approximations, yielded reproducible results.

Rigid body modeling was carried out by iterative rotation of each dimer of the structure (pdb id: 1FNY) to minimize the discrepancy with the SAXS camptosemin curve. The model was displayed using MASSHA (Konarev et al. 2001). Structural parameters from DAM, from dimer structure (pdb id: 1LOC; Bourne et al. 1994), from tetrameric structure (pdb id: 1FNY; Rabijns et al. 2001), and from the rigid body model were obtained with CRYSOL (Svergun et al. 1995). The superposition of the

crystallographic rigid body model and DAM structures was done using the program SUPCOMB (Kozin and Svergun 2001).

pH-Dependent structural changes

Camptosemin samples were incubated at room temperature in pH values ranging from 2.0 to 12.0 in 20 mM acetate-borate-phosphate buffers adjusted to the different pH values. In the intrinsic polarized fluorescence anisotropy assay, measurements were done with camptosemin at 0.54 μM in a 0.5 ml, 1-cm path length quartz cuvette, using a 280-nm excitation wavelength. The anisotropy was computed as the mean of ten measurements across each of the samples, under each set of conditions. All of the assays were carried out at 20°C. Camptosemin samples in the same pH range were subjected to SDS-PAGE analysis, without heating the samples prior to electrophoresis. For the static intrinsic fluorescence emission measurements, quartz cuvettes (0.5 ml, 1-cm light path length) were filled with 2.7 μM protein solutions and excited at 280 or 295 nm in a K2 ISS fluorimeter equipped with a temperature control system. The intensity of tryptophan fluorescence emission was monitored from 290–300 to 450 nm at different pHs (at 20°C). The buffer contributions were subtracted in all of the experiments.

Chemical unfolding

Chemical unfolding of camptosemin was monitored by far-UV CD spectroscopy (195–250 nm). The protein solutions used were 9.0 and 19.5 μM in 20 mM Tris-HCl buffer, pH 8.0, containing 20 mM NaCl at 20°C. Chemical denaturation was carried out by increasing the Gdm–HCl concentration from 0 to 7.7 M while monitoring the ellipticity change at 220 nm. The protein was incubated for 12 h in the corresponding buffer prior to measurements. All experiments were performed three times, and the buffer contribution was subtracted in all of the experiments. The fraction of denatured protein, f_d, was calculated from the relations:

$$f_d = \frac{(\theta_n - \theta_{obs})}{\theta_n - \theta_d} \quad \text{and } f_d + f_n = 1 \tag{1}$$

in which θ_{obs} is the ellipticity obtained at a particular Gdm-HCl concentration, and θ_d and θ_n are the values of the ellipticity characteristic of the denatured and native states, respectively. Chemical unfolding data were fit using a two-state homotetramer model (Johnson et al. 1995; Mallam and Jackson 2005), in which two populations of proteins, folded homotetramers (T) and unfolded monomers (M), exist at equilibrium.

Chemical unfolding was also monitored by intrinsic fluorescence spectroscopy. Native camptosemin at 4.5 and 10.0 μM, and at different Gdm-HCl concentrations (0–7.7 M) was used in all experiments. The experiments were carried out at least three times at 20°C, in 20 mM Tris-HCl buffer, pH 8.0, containing 20 mM NaCl. The fluorescence spectral center of mass (λ_{cm}) was calculated according to the equation:

$$\lambda_{cm} = \frac{\sum \lambda I(\lambda)}{\sum I(\lambda)} \tag{2}$$

where λ is the emission wavelength, and I(λ) represents the fluorescence intensity at wavelength λ (Lakowicz 1999).

Thermal unfolding monitored by CD spectroscopy

Thermal unfolding of native camptosemin was monitored by far-UV CD spectroscopy (208–250 nm). The camptosemin concentrations were approximately 4.5 and 19.5 μM in 20 mM Tris-HCl, 20 mM NaCl, pH 8. Thermal denaturation of native camptosemin, in the presence of 1.5 M Gdm–HCl, was characterized by measuring the change in ellipticity at 220 nm induced by a temperature increase from 20 to 95°C at a heating rate of 1°C min^{-1}.

Results and discussion

A new legume lectin was purified from crude extract of *C. ellipticum* seeds using a purification protocol that included two rounds of SEC on a Superdex-75 column, followed by ion exchange chromatography using a Mono-Q column. This procedure resulted in the separation of one major hemagglutinating fraction, shown in Fig. 1. The lectin, camptosemin, represented about 1.5% of the total protein found in the seeds (1.7 mg/g of seeds). Purified camptosemin migrated with the expected molecular mass of around 26 kDa, under reducing or non-reducing conditions after boiling on standard denaturing SDS-PAGE (insert, Fig. 1, columns 2 and 3). However, when the protein sample was subjected to SDS-PAGE without heating, it exhibited a larger size (insert, Fig. 1, columns 4 and 5), indicating that camptosemin is probably an oligomer in solution. These data are in agreement with other oligomeric lectins described in the literature (Almanza et al. 2004; Santos-de-Oliveira et al. 1994) and with the results described below.

The camptosemin primary sequence was deduced from its cDNA. The cDNA that encoded complete, mature camptosemin was amplified from the total seed RNA in two steps. The obtained sequence (GenBank accession number FJ392648) was submitted to the BLAST script, which retrieved sequence similarities with several legume lectin-related proteins; *Robinia pseudocacia* bark lectin (access no AB012635) had the highest score. The 5′

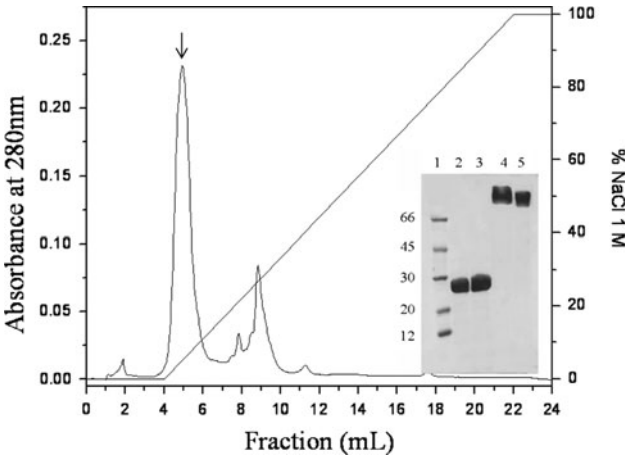

Fig. 1 Camptosemin elution profile from MonoQ 5/50 GL. *Dashed line* corresponds to NaCl gradient. Insert shows the major peak (indicated by the *arrow* in the chromatogram) eluted on SDS-PAGE: *lane 1*, molecular weight markes (kDa); boiled camptosemin in the presence (*lane 2*) and in the absence (*lane 3*) of β-mecaptoethanol; non-boiled camptosemin in the presence (*lane 4*) and in the absence (*lane 5*) of β-mecaptoethanol

obtained sequence revealed an N-terminal signal peptide when submitted to prediction by Signal-P (http://www.cbs.dtu.dk/services/SignalP/); furthermore, the predicted cleavage site agrees with the expectation based on N-terminal data previously obtained from Edman's degradation of the isolated protein. However, based on the lack of a 5′ start codon and on the length/sequence comparison with other legume lectin pre-peptides, the 5′-RACE information is still incomplete, missing some 5′ end information. Nevertheless, the primary structure of mature camptosemin could be deduced from the cloned sequences, which predict a mature protein with 243 amino acid residues, a molecular mass of 26 kDa (very close to the observed value for camptosemin under denaturing SDS–PAGE conditions), and a theoretical pI of 5.1 (Gasteiger et al. 2005). The deduced primary sequence was aligned using CLUSTAL-W and several legume lectin family members for similarity analysis and demonstrated extensive identities to *R. pseudocacia* bark lectin (57%; Fig. 2). Residues implicated in sugar binding were all conserved in camptosemin and were predicted by sequence similarities (Fig. 2; Loris et al. 1998; Rabijns et al. 2001).

Camptosemin bioassays applications

Camptosemin preferentially agglutinates erythrocytes from the O group. Comparing the carbohydrate-induced inhibition of agglutination displayed upon the addition of several sugars (Table 1), camptosemin activity was found to be affected most strongly by *N*-acetyl-D-galactosamine (MIC 0.015 M), followed by lactose (MIC 0.031 M), indicating its binding preferences. Camptosemin stimulates adhesion of the breast tumor cell line MDA-MB-231, promoting about 50% of the MDA-MB-231 cell adhesion observed in the positive control (collagen type I; Fig. 3). Cytometric analysis showed that MDA-MB-231 cells express high levels of the $\alpha 2\beta 1$ integrin (not shown), which is one of the major surface receptors for collagen I (Takada and Helmer 1989). However, these cells also have the ability to adhere to other proteins, such as fibronectin, and collagen III and IV. The adhesive properties of MDA-MB-231 cells can be related to their ability to invade and produce metastasis (Sheng et al. 1996). The adhesion of MDA-MB-231 cells was inhibited by the previous incubation with GalNAc. At 1:1 M ratio, no significant difference was observed. However, from molar ratios of 1:2 (camptosemin/GalNAc) up to 1:32, significant inhibition of cell adhesion could be observed. Increasing the GalNAc/camptosemin ratios did not significantly change this effect, and total inhibition was never achieved. Camptosemin probably acts as a cell adhesion molecule for MDA-MB-231 cells, binding GalNAc-glycoreceptors expressed in these tumor cells. Further studies must be done to determine if camptosemin could inhibit tumor cell motility and/or invasion.

Structural characterization of camptosemin

The quaternary structure of legume lectins leads to their ability to bind to glycoconjugates in a multivalent way at the cell surface. In this context, it has proven very helpful to use these molecules as model systems for investigation of the protein oligomerization process. Several approaches were used to determine the oligomerization state of the protein after purification and its quaternary structure. Together, SDS-PAGE, SEC, SAXS, and fluorescence anisotropy indicate that camptosemin purified as a homogeneous stable oligomer in the range of protein concentrations used in these experiments. Upon SEC, camptosemin eluted as a single peak of apparent molecular weight around 82 kDa; by SDS-PAGE, after camptosemin heat denaturation, an MW of approximately 26 kDa was observed (Figs. 4a and 1, respectively). Although most of the biophysical data appear to indicate a homotetrameric organization of the lectin, the data provided by SEC show a trimeric molecular weight. This apparent discrepancy might happen because of the lectin interaction properties of camptosemin with the polysaccharide column matrix. We observed a large delay when the SEC was performed without sugar (data not shown), which indicated that camptosemin, in fact, interacts with the polysaccharide matrix. Probably this interaction is not totally inhibited in the presence of 0.2 M lactose in the buffer, leading to the apparent discrepancy observed by SEC.

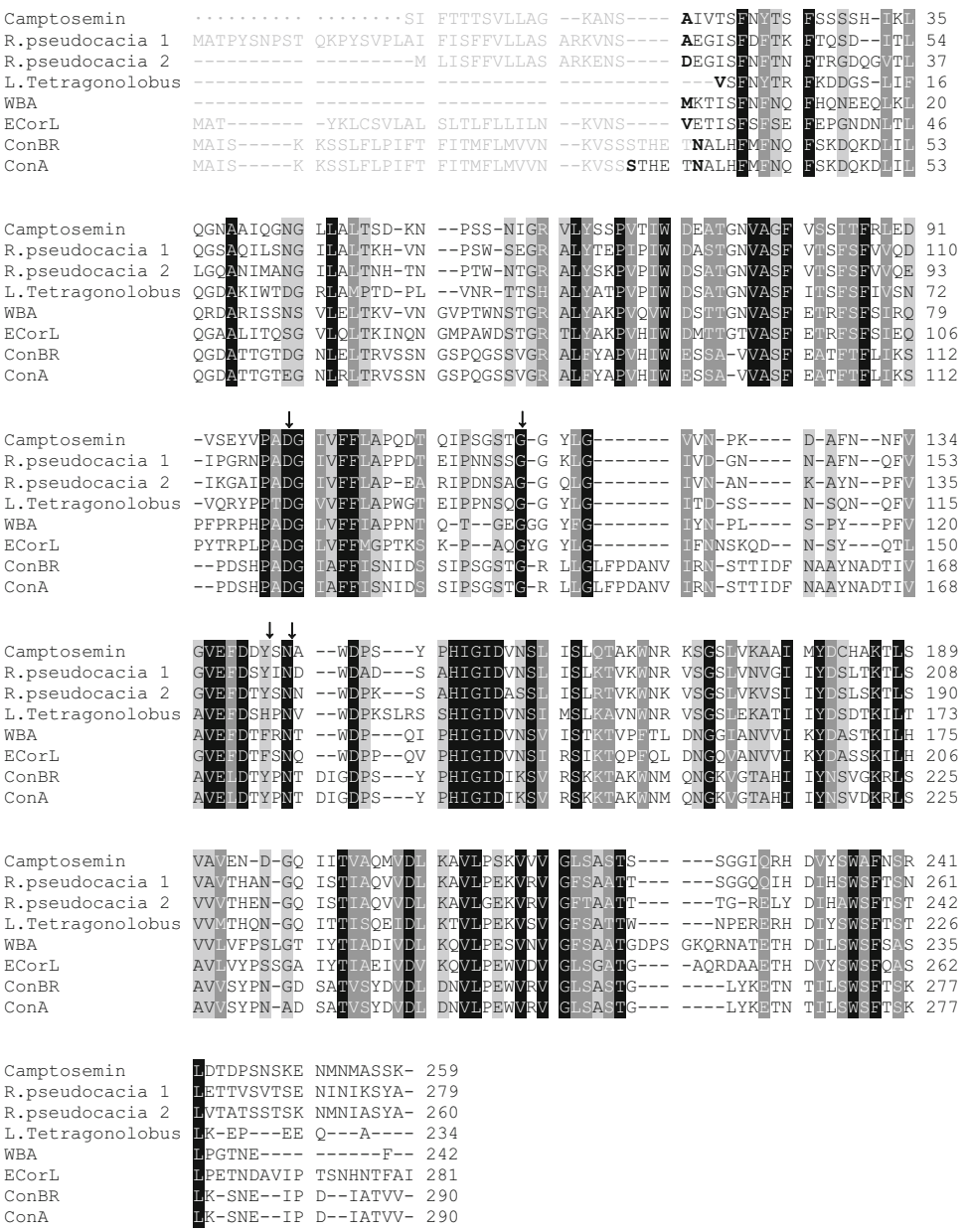

Fig. 2 Analysis of camptosemin primary sequence compared to several legume lectin family members. Identical residues among them are displayed in *black* background. Conservative substitutions are in *dark gray shading* and semi-conservative substitutions in *light gray* background. Residues lying within N-terminal signal peptides are in *light gray*, upstream of the first N-terminal residues (*bold faced*) of each mature protein sequence. Camptosemin N-terminal-missing residues are represented by *gray dots*. *Arrows* indicate probable residues implicated in sugar binding, predicted by sequence similarities (Loris et al. 1998; Rabijns et al. 2001). Camptosemin presents sequence identity ranging from 57 (*R. pseudocacia* 1) to 34% (ConBR and ConA) when compared to the other lectin sequences herein. Accession numbers for the sequences used are the following: *R. pseudocacia* 1, AB012635 (Yoshida and Tazaki 1999) *R. pseudocacia* 2, AAA80183 (Van Damme et al. 1995); *L.Tetragonolobus*, 2EIG_A (Moreno et al. 2008); WBA1, O24313 (Prabu et al. 1998); ECorL, CAA36986 (Arango et al. 1990); ConBR, CAA74202 (Grangeiro et al. 1997); ConA, CAA25787 (Carrington et al. 1985)

Taken together, the results were consistent with a homo-tetramer with an expected mass of around 104 kDa, confirmed by SAXS measurements. SAXS experimental scattering curves of camptosemin at 52 and 315 μM displayed the same profile, and since scattering curves at higher concentrations showed negligible interference effects, they were used in the SAXS analysis in the range of 0.03–2.35 nm^{-1} (Fig. 5a). Structural parameters derived from these curves are given in Table 2. Guinier plots of the obtained data exhibited linear profiles, indicating satisfactory monodispersity of camptosemin (Fig. 5a, insert). The pair distance distribution function $p(r)$ calculated from the GNOM fitted data is shown in Fig. 5b. These curves also provided the camptosemin maximum dimension (D_{max}), determined from the value of r for which the function $p(r)$ drops to zero. The determined camptosemin D_{max} was 9.5 ± 1.0 nm. The SAXS experimental curves were compared to the scattering intensity and the distance distribution $p(r)$ function calculated from the atomic coordinates of the dimeric and tetrameric lectin structure (Fig. 5a, b, respectively). Rigid body modeling was performed to obtain better agreement between camptosemin and a template (PDB id: 1FNY). The superposition of a crystallographic rigid body model and DAM structures was done using the program SUPCOMB (Fig. 5c). The curves, calculated from SAXS, and the radii of gyration, calculated from both the Guinier regions of the SAXS scattering curve (3.05 nm) and with the program GNOM (3.04 nm), are

Table 1 Inhibition of human O^+ erythrocyte agglutination

Carbohydrate	MIC (M)[a]	Relative activity
Sucrose	0.125	2
Lactose	0.031	8.1
Galactose	0.250	1
Methyl-α-D-galactopyranoside	0.125	2
Melibiose	0.125	2
N-acetyl-D-galactosamine	0.015	16.7

The erythroagglutination inhibitory activity of galactose was arbitrarily set as 1; 2.8 μM lectin was added to each well of the microtitration plate. The following sugars were not inhibitory at 125 mM: maltose, mannose, fucose, GlcNAc, maltose, methyl D-mannoside, D-(+)-raffinose, L-rhamnose

[a] Minimal inhibitory concentration

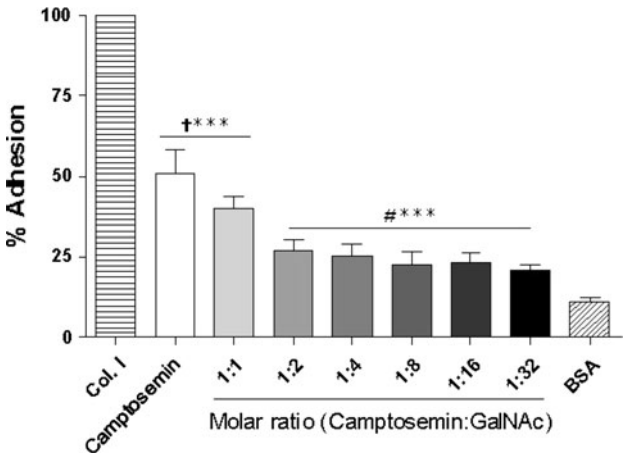

Fig. 3 Cell adhesion assay. GalNAc inhibits MDA-MB-231 breast cancer cell adhesion promoted by camptosemin. Camptosemin was incubated for 1 h at room temperature with GalNAc at molar ratios of 1:1 to 1:32 (camptosemin:GalNAc) in adhesion buffer, and 96-well plates were coated overnight at 4°C with this mixture. MDA-MB-231 cells labeled with CMFDA (1×10^6 cells/ml) were added to coated wells, and the plate was incubated for 30 min at 37°C. After washing the unbound cells, the bound cells were lysed by the addition of 0.5% Triton X-100, and plate was read in a fluorescence reader. BSA was used as a coating for negative control, and collagen type I (10 μg/ml) was used as a positive control for MDA-MB-231 cell adhesion. Values represent two independent experiments in triplicate, and data are expressed as percentage of control values on collagen type I, which represents 100% adhesion. Statistical analysis was performed using one-way analysis of variance (ANOVA), followed by the post hoc Bonferroni's test, $^{***}P < 0.001$, compared with the positive control (Col. I)

consistent with a homo-tetrameric structure in the form of a spherical-like molecule.

The oligomerization state of the protein was investigated by fluorescence anisotropy as a function of pH and temperature. Increasing temperatures induced larger values of anisotropy (Fig. 6a). Low anisotropic states ranging from pH 5 to pH 10 were observed. High anisotropic values were also observed in both extremely low pH (from pH 2 to pH 3.5) and highly alkaline pH (pH 12; Fig. 6a). The same samples were also monitored on SDS-PAGE, and monomeric forms were found in the extremely low and high pHs, whereas the tetramer was found within the intermediary pH range (Fig. 6b). Such behavior is similar to soybean agglutinin (SBA), a tetrameric legume lectin like camptosemin that retains its tetrameric identity very well until below pH 2.5, when the dissociation of tetramers into monomers begins to occur (Sinha and Surolia 2005). Fluorescence emission and CD data showed that incubation of camptosemin in a pH range from 2 to 10 did not significantly affect the shape of the CD spectrum or the maximum fluorescence emission wavelength (data not shown). All these data suggest the dissociation of the quaternary structure of camptosemin into subunits of smaller size (probably monomers). As evident from the CD spectra, monomers and tetramers are almost structurally unperturbed in the pH range 2–10, with a modest change at pH 12. Nevertheless, the hypothesis of local rearrangements of camptosemin monomers within the native tetramer cannot be excluded, and neither can the possibility that both local rearrangements, with tetramer shape change and tetramer to monomer dissociation, might co-exist. Additionally, the anisotropy values of camptosemin showed a gradual increase with increasing temperature (indicating that the size of camptosemin decreases when heated), but such values seem to be closer to the tetrameric camptosemin anisotropy than to the monomeric types seen in the pH-driven anisotropy experiment (Fig. 6).

The stability of camptosemin was also investigated as a function of chemical and thermal denaturant agents. Chemical denaturation was studied by intrinsic fluorescence emission at 20°C. Figure 7a (solid line) shows the fluorescence emission spectra of camptosemin in the absence of Gdm–HCl. An emission maximum at approximately 332 nm was observed, typical of tryptophan residues buried inside a solvent-inaccessible protein core. However, at high Gdm-HCl concentration (~7 M), the results indicate that tryptophan residues should be solvent-exposed due to a significant bathochromic red-shift of the fluorescence emission maximum (from 332 to 352 nm). Also, severe quenching of the fluorescence emission intensity could be detected, which indicates that camptosemin in this environment could be a completely unfolded protein. The fluorescence quenching observed in denaturation conditions, in contrast with native camptosemin, is possibly due to collisional quenching by the solvent. Also, a different chemical environment, such as a salt bridge between acid and basic residues, may act to quench of its emission. In Fig. 7b, the unfolded fraction of camptosemin, calculated from the center of mass of the fluorescence spectrum, is shown as a function of Gdm-HCl concentration (see "Materials and methods"). This curve

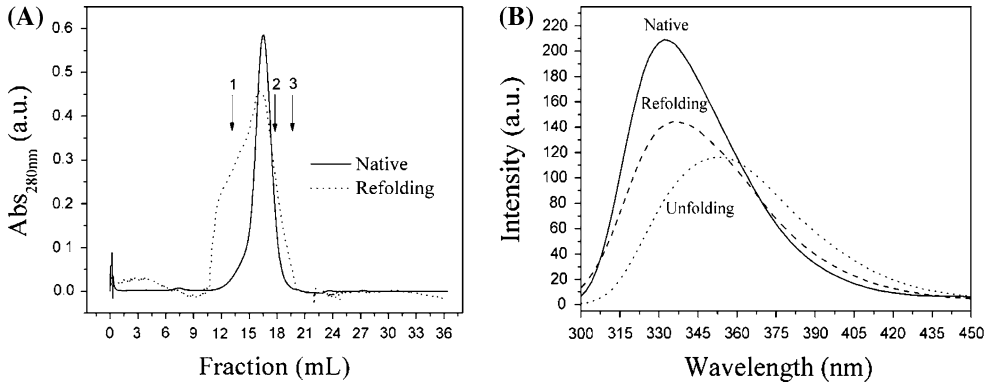

Fig. 4 Size exclusion chromatography (SEC) and tryptophan fluorescence emission of native, unfolding and refolded forms. **a** Size exclusion profile of native (108 μM) and refolded (in the same concentration) camptosemin performed in Superdex-200 column, equilibrated with 20 mM Tris–HCl, pH 8 buffer containing 0.2 M lactose, 0.3 M NaCl. The *arrows* indicate the elution volume of the standards: (1) β-amylase (200 kDa), (2) carbonic anhydrase (30 kDa), and (3) cytochrome C (12 kDa). **b** Fluorescence spectra of camptosemin in native, unfolded and refolded states. The spectra of native and refolded protein were taken using 6 μM of the fractions from Superdex-200 elution, at 20°C with a 1-cm optical path length cuvette. Samples were excited at 295 nm and emission intensity scanned from 300 to 450 nm

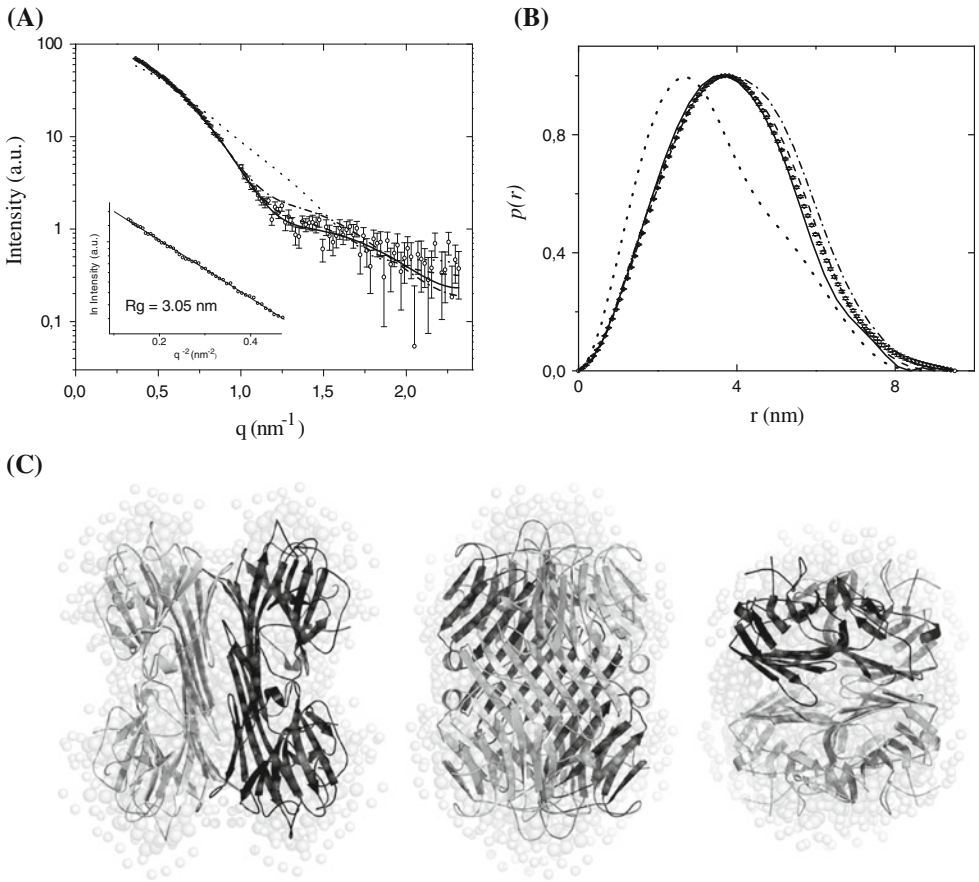

Fig. 5 SAXS measurements. **a** SAXS curve of the camptosemin protein superimposed with the theoretical scattering curve from the low-resolution model. The radius of gyration obtained from the Guinier plot (insert) is $R_g = 3.05$ nm, which is very close to the value of $R_g = 3.04$ nm obtained from the integral analysis of the scattering curve using the method implemented in GNON. **b** Distance distribution, $p(r)$, of camptosemin computed by indirect Fourier transform with GNON. **c** Three orthogonal views of the camptosemin "ab initio" DAM superposed with the tetrameric rigid body model from template structure (PDB id:1FNY). The figure was prepared using PyMOL (DeLano Scientific, San Carlos, CA; http://www.pymol.org)

suggests that there are no detectable amounts of intermediate states present (two-state transition) during the chemical unfolding process.

The secondary structure of camptosemin was probed by CD spectroscopy. Both CD and fluorescence experiments were done at the comparable protein concentrations (see Table 3). The CD spectrum was characterized by a minimum at approximately 223 nm and a maximum at approximately 195 nm (Fig. 7c, solid line, Gdm-HCl 0 M), compatible with the expectations for a typical legume lectin. The CLUSTER script classified camptosemin as an all β-class protein, similar to the tertiary structure of other

Table 2 Structural parameters of SAXS

Sample parameter	52 μM	315 μM	Dam[a]	1LOC[b]	1FNY[b]	RBM[c]
R_g (nm)	3.05 ± 0.50	3.00 ± 0.50	2.59	2.51	2.90	2.83
D_{max} (nm)	9.50 ± 1.00	9.50 ± 1.00	9.00	8.9	9.55	9.30
Discrepancy χ^d	–	–	1.09	10.70	1.90	1.13
Resolution (nm)	3.18	2.73	–	–	–	–
Volume (nm^3)	–	–	135.9	72.07	128.10	148.50

Exp., calculated from the experimental data

[a] DAM, parameters from the dummy atoms models averaged over ten models

[b] PDB, parameters from crystallographic model of pdb id: 1LOC and pdb id: 1FNY, respectively

[c] RBM, parameters from the rigid body model

[d] The data were compared with experimental parameters of camptosemin 462 μM

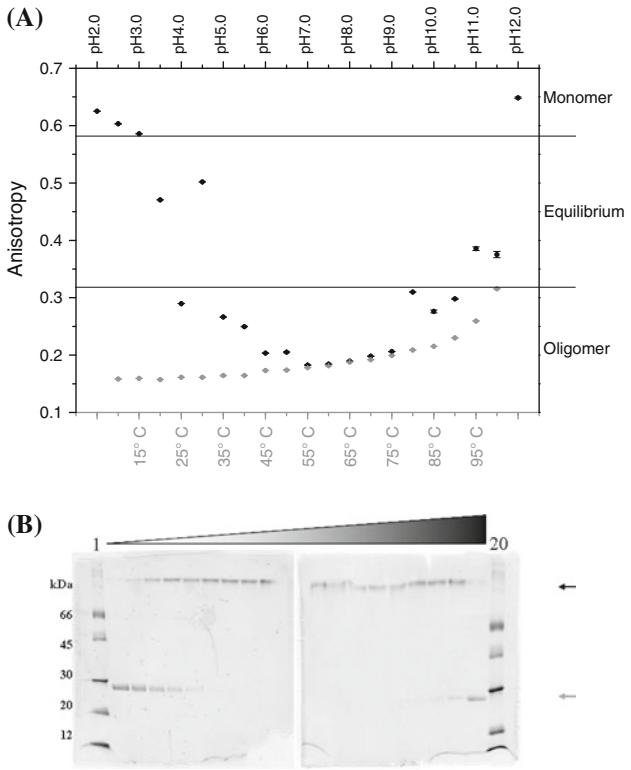

Fig. 6 Polarized fluorescence anisotropy. **a** Camptosemin samples at 0.54 μM were submitted to polarized fluorescence anisotropy determination under 280 nm excitation wavelength. Measurements are represented as the mean value of ten consecutive scans trough the samples. Polarized fluorescence anisotropy along thermal denaturation is in *gray*. Polarized fluorescence anisotropy of camptosemin in different pHs is in *black*. **b** SDS-PAGE of camptosemin in different pHs. *Lane 1 and 20* molecular mass standards. *Left panel* samples in the pH range from 2 to 6 in 0.5 subdivisions. *Right panel* samples in the pH range from 8 to 12 in 0.5 subdivisions. pH gradation is shown above the figure, indicating lower pH values in *white* and higher ones in *dark*. A *black arrow* indicates camptosemin oligomer and a *gray* one the monomer

legume lectins (Rabijns et al. 2001). A well-suited test for a two-state transition hypothesis is to examine whether changes in the secondary structure (CD method) occur simultaneously with modifications to the tertiary structure (fluorescence method). When the secondary structure of camptosemin was examined by far-UV CD spectroscopy as a function of Gdm–HCl, the changes were coincident with the intrinsic fluorescence emission. At 7 M Gdm-HCl, the far-UV CD spectrum of camptosemin is characteristic of a denatured unfolded protein (Fig. 7c). Monitoring the CD spectrum at 220 nm, a sigmoidal-like transition similar to that obtained by the fluorescence emission spectral center of mass method was found (Fig. 7d); this suggests that no folding intermediate species accumulated during the denaturation process.

The curves of normalized fluorescence and CD-monitored unfolding of camptosemin against Gdm–HCl concentrations could almost be superimposed (Fig. 7e), so they could be fitted, individually or together, to a reversible two-state unfolding/refolding model equation, indicating that camptosemin behaves as a single cooperative unit upon chemical denaturation. The unfolding curves measured by the two methods give the same value of approximately 4 M for the $[Gdm–HCl]_{1/2}$.

Upon refolding, fluorescence emission showed partial reversibility of the unfolding process (Fig. 4b). Refolding experiments using SEC also confirmed the partial reversibility of the process (Fig. 4a). Camptosemin exhibited about 70% reversibility upon refolding of the protein unfolded by Gdm–HCl denaturation. Thus, all results indicated that the unfolding of camptosemin appears to be a two-state mechanism. Because of this, the analysis of the denaturation curves was performed with the assumption that only two states (the native and the unfolded) exist at equilibrium. This assumption may not always be true for oligomeric proteins, and it would also depend upon the contribution of inter-subunit interactions to the total protein stability. In the denaturation process, the formation of partially folded intermediates is possible. In the present study, the denaturation curves of camptosemin monitored by far-UV CD and fluorescence were cooperative and

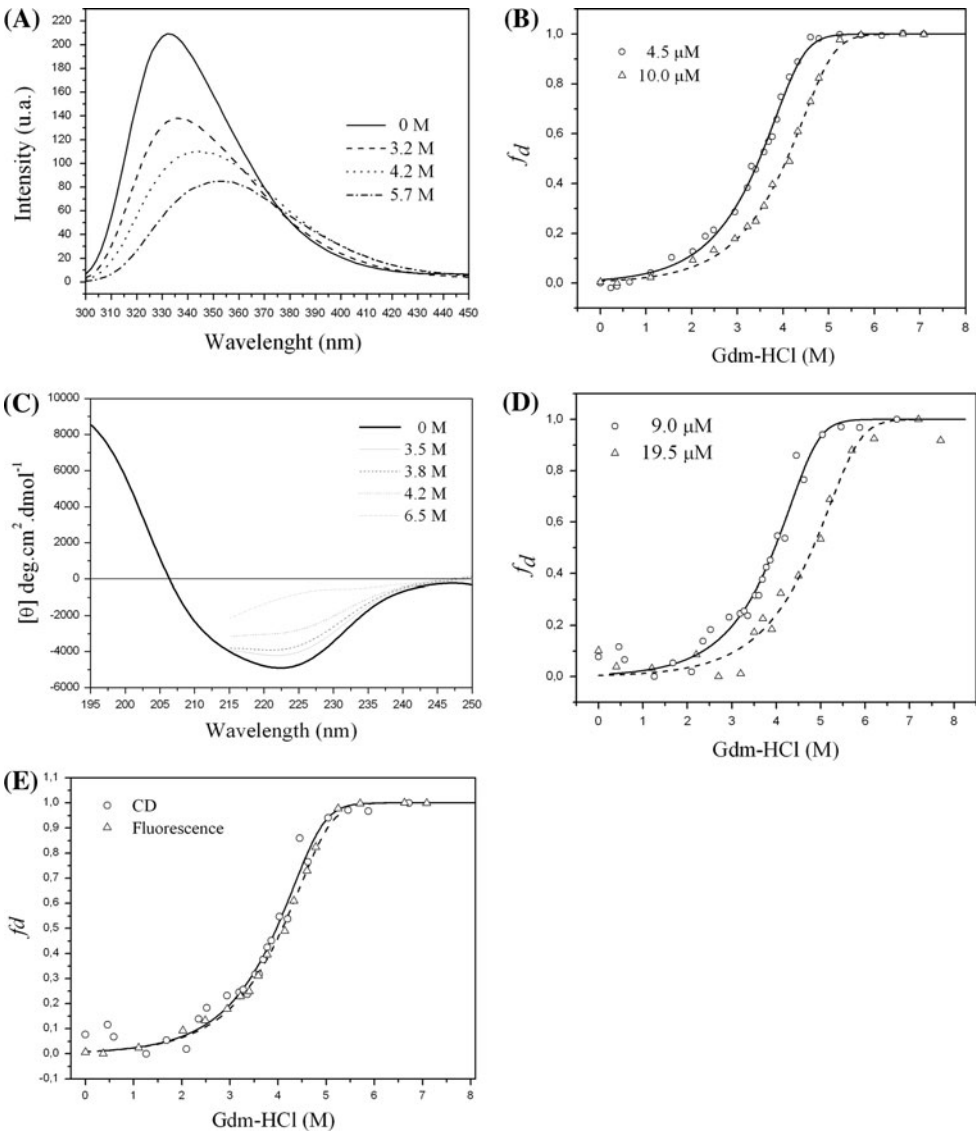

Fig. 7 Chemical unfolding of camptosemin. **a** Gdm-HCl induced unfolding of camptosemin (4.5 μM) monitored by fluorescence. **b** Gdm-HCl denaturation curves of camptosemin (4.5 and 10 μM) monitored by fluorescence following the displacement of the mass center and expressed in terms of denatured protein fraction as a function of guanidine-HCl concentration. **c** Gdm-HCl induced unfolding of camptosemin (9 μM) monitored by far-UV CD. **d** Gdm-HCl denaturation curves of camptosemin (9 and 19.5 μM) monitored at 220 nm by far-UV CD and expressed in terms of denatured protein fraction as a function of Gdm–HCl concentration. **e** Comparison curves of camptosemin chemical denaturation by circular dichroism and fluorescence. The CD and fluorescence measurements were done with camptosemin 9 and 10 μM, respectively

Table 3 Thermodynamic parameters from the fit of camptosemin in a two-state model

Pt (μM)	Far-UV CD			Pt (μM)	Fluorescence		
	$[D]_{50\%}$ (M Gdm–HCl)	$m_{n_4 \leftrightarrow 4D}$ (KJ mol$^{-1}{}_{\mathrm{M}}^{-1}$)	$\Delta G^{N_4 \leftrightarrow 4D}_{H_2O}$ (KJ mol^{-1})		$[D]_{50\%}$ (M Gdm–HCl)	$m_{n_4 \leftrightarrow 4D}$ (KJ mol^{-1}M^{-1})	$\Delta G^{N_4 \leftrightarrow 4D}_{H_2O}$ (KJ mol^{-1})
9.0	3.9 ± 0.5	10.6 ± 0.6	126.0 ± 0.1	4.5	3.5 ± 0.1	10.7 ± 0.3	129.7 ± 0.1
19.5	4.8 ± 0.1	9.8 ± 0.7	128.6 ± 0.1	10.0	4.1 ± 0.1	10.3 ± 0.2	128.7 ± 0.1

Concentration in terms of camptosemin monomers

super-imposable (Fig. 7e), suggesting the existence of only two species in the transition. Similar behavior has been observed in the chemical unfolding-folding process for concanavalin A (Sinha et al. 2005) and SBA lectin (Sinha and Surolia 2005).

The data from Fig. 7b, d were analyzed (at different protein concentrations) using a two-state model in which two protein populations, folded homotetramers (T) and unfolded monomers (M), exist at equilibrium. The protein concentration (P_t)-dependence of equilibrium unfolding curves in homotetramer systems is expected, and it can be understood from the definition of the equilibrium constant K_U: $K_U = [M]^4/[T]$. At a given denaturant concentration, K_U and ΔG remained constant for all protein concentrations, and only the fraction of each equilibrium species presented changes with P_t. In a homotetramer system,

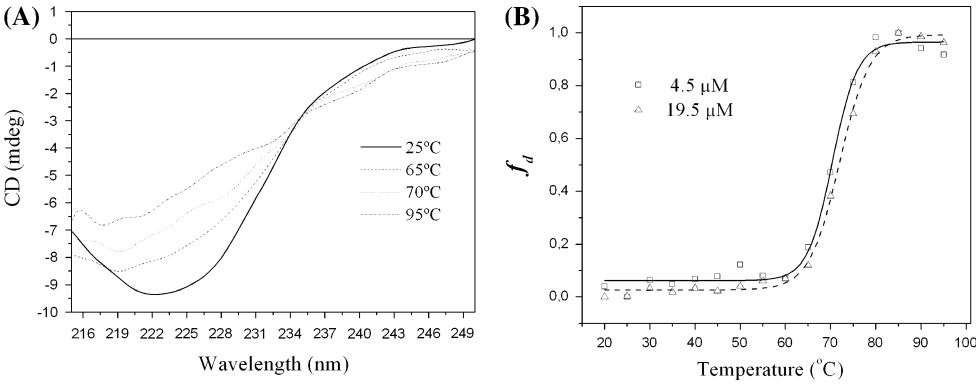

Fig. 8 Thermal unfolding of camptosemin. **a** Thermal-induced unfolding of camptosemin monitored by far-UV CD. **b** Thermal denaturation curves of camptosemin (4.5 and 19.5 μM), monitored at 220 nm, by far-UV CD, expressed in terms of denatured protein fraction as a function of temperature

$[U]_{1/2}$ is defined as the concentration of denaturant such that the fraction of unfolded monomers is equal to the fraction of monomers presenting as tetramers. This is also when $K_U = 0.5\ P_t^3$; therefore, the concentration of denaturant corresponding to $[U]_{1/2}$ will depend on P_t, and a change in $[U]_{1/2}$ with the total protein concentration is expected. $\Delta G_{H_2O}^{T_4 \leftrightarrow 4D}$ remains the same with changing P_t and $[U]_{1/2}$. The m value is a constant for each protein and should not be affected by protein concentration. When camptosemin unfolding data were analyzed according to a two-state denaturation model, the $m_{T_4 \leftrightarrow 4D}$ and $\Delta G_{H_2O}^{T_4 \leftrightarrow 4D}$ values remained the same for all concentrations of the protein (see Table 3). The $\Delta G_{H_2O}^{T_4 \leftrightarrow 4D}$ value determined here was approximately 130 kJ/mol (31 kcal/mol), very close to the value obtained for the protein concanavalin A (Sinha et al. 2005). Thus, a two-state homotetramer model described the experimental results adequately. However, it is possible that the tetramer form of camptosemin can dissociate, producing dimers or monomers before reaching the denatured state, but these forms could not be detected by the methods used in the present work.

Finally, the thermal stability, in the presence of 1.5 M Gdm–HCl, of camptosemin was monitored by far-UV CD in the range of 20–95°C (Fig. 8a, b). Native camptosemin could not be completely thermally unfolded in the absence of a chemical denaturant. The data showed that camptosemin was stable up to 60°C with a T_m point at 71°C, and also suggested a two-state model for the thermal denaturation. When the temperature was increased from 70 to 90°C, the intrinsic fluorescence emission of camptosemin exhibited a significant bathochromic shift of its maximum, from 332 to 338 nm, indicating the exposure of tryptophan residues to the buffer (data not shown). These data indicate that camptosemin is a heat resistant protein, similar to some other members of the legume lectin family (Srinivas et al. 2001). However, in contrast to the Gdm–HCl-induced denaturation process, the thermal denaturation of camptosemin was found to be an irreversible process, since samples that were heated up to 95°C did not return to their original state after either rapid or slow cooling back to 20°C.

Conclusion

In this study, a new protein isolated from *C. ellipticum* seeds is described. It is characterized as *N*-acetyl-D-galactosamine-binding lectin and named camptosemin. Structural studies using SAXS and SEC show that camptosemin forms a homo-tetrameric assembly, with a spherical shape. Structural characterization indicates that equilibrium unfolding/refolding of native camptosemin induced by Gdm-HCl proceeds through a reversible, classical two-state homotetrameric mechanism, without the accumulation of intermediate states. In addition, camptosemin is stable over a wide pH range [4–11].

We also demonstrated that this protein acts as a cell adhesion molecule for MDA-MB-231 tumor cells, an effect mediated by its sugar-binding property, since the adhesion process was partially inhibited by a specific monosaccharide. These results suggest new studies to clarify if camptosemin can inhibit the motility and/or invasion of the tumor cells.

Acknowledgments The authors are very grateful to Dr. Lúcia Rossi for botanical identification work carried out at the Botanical Institute, São Paulo, Brazil.

References

Almanza M, Vega N, Pérez G (2004) Isolating and characterizing a lectin from *Galactia lindenii* seeds that recognises blood group H determinants. Arch Biochem Biophys 429:180–190

Altschul SF, Madden TL, Schäffer AA, Zhang J, Zhang Z, Miller W, Lipman DJ (1997) Gapped BLAST and PSI-BLAST: a new generation of protein database search programs. Nucleic Acids Res 25:3389–3402

Arango R, Rozenblatt S, Sharon N (1990) Cloning and sequence analysis of the *Erythrina corallodendron* lectin cDNA. FEBS Lett 264:109–111

Bourne Y, Ayouba A, Rouge P, Cambillau C (1994) Interaction of a legume lectin with two components of the bacterial cell wall; a crystallographic study. J Biol Chem 269:9429–9435

Brinda KV, Mitra N, Surolia A, Vishveshwara S (2004) Determinants of quaternary association in legume lectins. Protein Sci 13:1735–1749

Campana PT, Moraes DI, Moteiro-Moreira ACO, Beltramini LM (2002) Unfolding and refolding studies of frutalin, a tetrameric D-galactose binding lectin. Eur J Biochem 269:753–758

Carrington DM, Auffret A, Hanke DE (1985) Polypeptide ligation occurs during post-translational modification of concanavalin A. Nature 313:64–67

Chatterjee A, Mandal DK (2003) Denaturant-induced equilibrium unfolding of concanavalin A is expressed by a three-state mechanism and provides an estimate of its protein stability. Biochim Biophys Acta 1648:174–183

Chatterjee A, Mandal DK (2005) Quaternary association and reactivation of dimeric concanavalin A. Inter J Biol Macromol 35:103–109

Cominetti MR, Terruggi CH, Ramos OH, Fox JW, Mariano-Oliveira A, de Freitas MS, Figueiredo CC, Morandi V, Selistre-De-Araujo HS (2004) Alternagin-C, a disintegrin-like protein, induces vascular endothelial cell growth factor (VEGF) expression and endothelial cell proliferation in vitro. J Biol Chem 279:18247–18255

Frohman MA, Dush MK, Martin GR (1988) Rapid production of full-length cDNAs from rare transcripts: amplification using a single gene-specific oligonucleotide primer. Proc Natl Acad Sci USA 85:8998–9002

Gasteiger E, Hoogland C, Gattiker A, Duvaud S, Wilkins MR, Appel RD, Bairoch A (2005) Protein identification and analysis tools on the ExPASy server. In: Walker JM (ed) The proteomics protocols handbook. Humana Press, Totowa, pp 571–607

Gatehouse AMR, Powell KS, Van Damme EJM, Peumans WJ (1995) Insecticidal properties of plant lectins their potential in plant protection. In: Pustzai A, Bardocz S (eds) Lectins: biomedical perspectives. Taylor and Francis, London, pp 35–58

Grangeiro TB, Schriefer A, Calvete JJ, Raida M, Urbanke C, Barral-Netto M, Cavada BS (1997) Molecular cloning and characterization of ConBr, the lectin of *Canavalia brasiliensis* seeds. Eur J Biochem 248:43–48

Johnson CR, Morin PE, Arrowsmith CH, Freire E (1995) Thermodynamic analysis of the structural stability of the tetrameric oligomerization domain of p53 tumor suppressor. Biochem 34:5309–5316

Konarev PV, Petoukhov MV, Svergun DI (2001) MASSHA–a graphics system for rigid-bodymodelling of macromolecular complexes against solution scattering data. J Appl Cryst 34:527–532

Kozin MB, Svergun DI (2001) Automatedmatching of high- and low-resolution structural models. J Appl Cryst 34:33–41

Laemmli UK (1970) Cleavage of structural proteins during the assembly of the head of bacteriophage T4. Nature 227:680–685

Lakowicz JR (1999) Principles of fluorescence spectroscopy, 2nd edn. Plenum Publishers, New York

Larkin MA et al (2007) ClustalW and ClustalX version 2. Bioinformatics 23:2947–2948

Loris R, Hamelryck T, Bouckaert J, Wyns L (1998) Legume lectin structure. Biochim Biophys Acta 1383:9–36

Mallam AL, Jackson SE (2005) Folding studies on a knotted protein. J Mol Biol 346:1409–1421

Moreno FB, de Oliveira TM, Martil DE, Vicoti MM, Bezerra GA, Abrego JR, Cavada BS, Filgueira AJ (2008) Identification of a new quaternary association for legume lectins. J Struct Biol 161:133–143

Petoukhov MV, Svergun DI (2003) New methods for domain structure determination of proteins from solution scattering data. J Appl Cryst 36:540–544

Prabu MM, Sankaranarayanan R, Puri KD, Sharma V, Surolia A, Vijayan M, Suguna K (1998) Carbohydrate specificity and quaternary association in basic winged bean lectin: X-ray analysis of the lectin at 2.5 Å resolution. J Mol Biol 276: 787–796

Rabijns A, Verboven C, Rougé P, Barre A, Van Damme EJM, Peumans WJ, De Ranter CJ (2001) Structure of a legume lectin from the bark of *Robinia pseudoacacia* and its complex with N-Acetylgalactosamine. Proteins Structure Funct Bioinform 44:470–478

Rüdiger H, Gabius HJ (2001) Plant lectins: occurrence, biochemistry, functions and applications. Glycoconjugate J 18:589–613

Sanger F, Nicklen S, Coulson AR (1977) DNA sequencing with chain-terminating inhibitors. Proc Natl Acad Sci USA 74:5463–5467

Santos-de-Oliveira R, Dias-Baruffi M, Thomaz SM, Beltramini LM, Roque-Barreira MC (1994) A neutrophil migration-inducing lectin from *Artocarpus integrifolia*. The J Immunol 153:1798–1807

Sharon N (2007) Lectins: carbohydrate-specific reagents and biological recognition molecules. J Biol Chem 282:2753–2764

Sharon N, Lis H (1990) Legume lectins—a large family of homologous proteins. FASEB J 4:3198–3208

Sharon N, Lis H (2004) History of lectins: from hemagglutinins to biological recognition molecules. Glycobiol 14:53–62

Sheng S, Carey J, Seftor EA, Dias L, Hendrix MJ, Sager R (1996) Maspin acts at the cell membrane to inhibit invasion and motility of mammary and prostatic cancer cells. Proc Natl Acad Sci USA 93:11669–11674

Sinha S, Surolia A (2005) Oligomerization endows enormous stability to soybean agglutinin: a comparison of the stability of monomer and tetramer of soybean agglutinin. Biophys J 88:4243–4251

Sinha S, Mitra N, Kumar G, Bajaj K, Surolia A (2005) Unfolding studies on soybean agglutinin and concanavalin a tetramers: a comparative account. Biophys J 88:1300–1310

Sreerama N, Venyaminov SY, Woody RW (2001) Analysis of protein CD spectra with a reference protein set based on tertiary structure class. Anal Biochem 299:271–274

Srinivas VR, Reddy GB, Ahmad N, Swaminathan CP, Mitra N, Surolia A (2001) Legume lectin family, the "natural mutants of the quaternary state", provide insights into the relationship between protein stability and oligomerization. Biochim Biophys Acta 1527:102–111

Svergun DI (1992) Determination of the regularization parameter in indirect-transform methods using perceptual criteria. J Appl Crystallogr 25:495–503

Svergun DI, Semenyuk AV, Feigin LA (1988) Small angle-scattering-data treatment by the regularization method. Acta Crystallogr A 44:244–250

Svergun D, Barberato C, Koch MHJ (1995) CRYSOL—a program to evaluate X-ray solution scattering of biological macromolecules from atomic coordinates. J Appl Cryst 28:768–773

Svergun DI, Petoukhov MV, Koch MH (2001) Determination of domain structure of proteins from X-ray solution scattering. Biophys J 80:2946–2953

Takada Y, Helmer ME (1989) The primary structure of the VLA-2/collagen receptor alpha 2 subunit (platelet GPIa): homology to other integrins and the presence of a possible collagen-binding domain. J Cell Biol 109:397–407

Van Damme EJ, Barre A, Smeets K, Torrekens S, Van Leuven F, Rouge P, Peumans WJ (1995) The bark of *Robinia pseudoacacia* contains a complex mixture of lectins. Characterization of the proteins and the cDNA clones. Plant Physiol 107:833–843

Van Damme EJM, Peumans WJ, Barre A, Rougé P (1998) Plant lectins: a composite of several distinct families of structurally and evolutionary related proteins with diverse biological roles. Crit Rev Plant Sci 17:575–692

Varela ED, Lima JPMS, Galdino AS, Pinto LS, Bezerra WM, Nunes EP, Alves MAO, Grangeiro TB (2004) Relationships in subtribe diocleinae (Leguminosae; Papilionoideae) inferred from internal transcribed spacer sequences from nuclear ribosomal DNA. Phytochem 65:59–69

Yoshida K, Tazaki K (1999) Expression patterns of the genes that encode lectin or lectin-related polypeptides in *Robinia pseudoacacia*. Aust J Plant Physiol 26:495–502